

the highest occupied molecular orbital, i.e., a sulfur lone-pair orbital nearly perpendicular to the  $R_1, S, R_2$  plane. Conversely, nucleophiles tend to approach along the direction of the lowest unoccupied molecular orbital, i.e.,  $\sigma^*(S-R_1)$  or  $\sigma^*(S-R_2)$ .<sup>46</sup>

### Concluding Remarks

This Account illustrates the variety of chemical phenomena that can be investigated by systematic examination of published crystallographic results. Such analyses can now be carried out with comparative ease by both crystallographers and chemists. Although there is much scepticism about the relevance of crystallographic results to molecular properties in solution, this Account shows that this reservation has only limited justification. The reaction pathway studies, in particular, demonstrate that crystal-packing effects are small enough to permit meaningful analysis of very weak interactions, such as  $N \cdots C=O$  and  $O \cdots C=O$ .

(46) For other reaction pathway studies, see: Bürgi, H. B. *Inorg. Chem.* 1973, 12, 2321-2325. Bürgi, H. B. *Angew. Chem., Int. Ed. Engl.* 1975, 14, 460-473. Britton, D.; Dunitz, J. D. *Helv. Chim. Acta* 1980, 63, 1068-1073.

The 30 000 organocarbon crystal structures currently available cover an enormous chemical range and include many novel and unusual compounds (since these are the ones most likely to be examined by crystallographic methods). By the end of the century, there will be over 100 000 structures in the public domain. The importance of this information to organic chemistry can scarcely be overstated, because the results of most crystal structure determinations are precise, detailed, and unambiguous. However, studies of individual structures are often of limited value: if an unexpected structural feature is observed, it may not be statistically significant and may well be ascribed to experimental errors or packing effects. When the same feature is consistently observed in a series of related structures, these explanations become untenable and the observation must be rationalized in physicochemical terms. Thus, the *systematic* analysis of large numbers of related structures is a powerful research technique, capable of yielding results that could not be obtained by any other method.

We thank Professors Aldo Domenicano and Jack Dunitz for reading the manuscript prior to submission.

## From Crystal Statics to Chemical Dynamics

HANS BEAT BÜRGI\*

Laboratory for Chemical and Mineralogical Crystallography, University of Berne, CH-3012 Berne, Switzerland

JACK D. DUNITZ\*

Organic Chemistry Laboratory, Swiss Federal Institute of Technology, CH-8092 Zürich, Switzerland

Received May 19, 1982 (Revised Manuscript Received October 6, 1982)

The study of molecular structure involves both static and dynamic aspects, the static aspects dealing with equilibrium arrangements of atoms in molecules, the dynamic ones with the relative motion of atoms during molecular vibrations or transformations, i.e., chemical reactions. The contribution of X-ray crystallography to the static aspects is well-known; in fact, for many years now, crystallography has been the main source of our information about the three-dimensional structure of molecules.<sup>1</sup> Automatic diffractometers and fast, powerful methods for interpreting the diffraction measurements have led to an unprecedented increase in the amount of structural information available.<sup>2</sup> Fortunately, for organic structures at least, this information is stored in computer-readable form in the Cambridge Structural Database (CSD), which has es-

tablished itself as an essential instrument for answering questions about the systematics of atomic arrangements in molecules.<sup>3</sup>

It is not so well-known that crystallography can also provide important information about the dynamic aspects of molecular structure. Of course, we cannot observe the actual motion of the atoms; an X-ray diffraction experiment takes roughly  $10^5$ - $10^6$  s, whereas dynamic processes on the molecular level occur on a time scale of  $10^{-12}$  s or less. Thus, diffraction measurements provide at best averaged information, in the form of mean-square vibration amplitudes for the individual atoms (expectation values of the square of the atomic displacements from equilibrium). This is the kind of information that is expressed in vivid, pictorial fashion by the thermal ellipsoids in the computer-drawn ORTEP diagrams that adorn many crystallographic publications.<sup>4</sup> At a given temperature, large extension

Hans-Beat Bürgi was born in Switzerland in 1942. He studied chemistry and received his Ph.D. degree at the ETH, Zürich, working with Jack D. Dunitz at the Laboratory for Organic Chemistry. After 2 years as a postdoctoral student of Larry S. Bartell at the University of Michigan, he joined the Laboratory for Inorganic Chemistry, ETH, Zürich. In 1979 he became Professor of X-ray crystallography at the University of Berne, Switzerland.

Jack D. Dunitz was born in Glasgow in 1923 and studied chemistry at Glasgow University, where he received his B.Sc. and Ph.D. degrees. Following a decade of postdoctoral studies at Oxford, Caltech, NIH, and the Royal Institution, London, he moved in 1957 to the ETH, Zürich, where he has been ever since and where he is Professor of Chemical Crystallography.

(1) J. D. Dunitz, "X-Ray Analysis and the Structure of Organic Molecules", Cornell University Press, Ithaca, NY, 1979.

(2) As of early 1982 the number of published organic crystal structures was more than 30 000 and increasing at the rate of about 4000 per year. Corresponding figures for inorganic structures are not known to us.

(3) For a recent authoritative review, see F. H. Allen, O. Kennard, and R. Taylor, *Acc. Chem. Res.*, preceding paper in this issue. See also the editorial by J. P. Glusker, *Acc. Chem. Res.*, 15, 231 (1982).

of the ellipsoid implies a large amplitude of motion of the atom in question in that direction and hence a shallow local potential. Less vivid, but necessary for quantitative evaluation, are the components  $U^{ij}$  (along the reciprocal base vectors) of the atomic vibration tensors  $U$ . The mean-square amplitude in any direction is then given by  $l^T U l$ , where  $l$  is a unit vector referred to the same base vectors.<sup>1,5</sup> The importance of atomic vibration tensors for testing lattice-dynamical calculations has been recognized for many years.<sup>6</sup> We shall show later how such information can also throw light on the details of certain kinds of molecular transformation.

A less direct but possibly more general approach to extracting dynamic information from crystallographic data is known as the structure-correlation method. The structure of a molecule in a crystal environment is not necessarily identical with the equilibrium structure of the isolated molecule, i.e., the forces exerted by a crystal environment can deform a molecule to a greater or lesser extent. Similarly, we expect that the structure of a given molecular fragment will depend to some extent on the particular molecules in which the fragment is embedded, as well as on the crystal environments.

In the structure-correlation method we are not interested in the forces as such, only in the deformations. We collect as many structures as possible containing the molecule or structural fragment of interest. Each structure provides, as it were, a snapshot of the fragment in a particular environment, and we try to order these into a sequence corresponding to a gradual deformation of the fragment. Each copy of the fragment is thus regarded as having been "frozen" by its particular environment.

One normally thinks of the molecule or structural fragment as a three-dimensional object. It is, however, conceptually useful to represent it instead as a point in a many-dimensional space, one dimension for each variable structural parameter.<sup>7</sup> Thus, an ensemble of frozen-in fragments is represented by a distribution of points (sample points). The advantage of this kind of

(4) C. K. Johnson, ORTEP, Report ORNL-5138, Oak Ridge National Laboratory, Oak Ridge, TN, 1976.

(5) The bad reputation associated with atomic vibration tensors from X-ray analysis is not justified as far as recent analyses are concerned, or, at any rate, not as justified as it used to be. Often in the past anisotropic vibrational parameters merely accumulated the systematic errors of the diffraction experiment and the inadequacies of the model including disorder, or they served to increase the number of adjustable parameters and to decrease the  $R$  value at the expense of a poor observation-to-parameter ratio. Today, many careful routine analyses account better for these deficiencies and can give physically significant information. Results based on extensive, accurate high-order data are quite comparable to those from neutron-diffraction studies. There is an ironical twist to the circumstance that most of the atomic tensors to be found in the literature are of poor quality, for just about the time that routine analyses began to produce physically interesting  $U^{ij}$  values the numbers began to disappear from the printed page. The volume of information was increasing so fast that many journals, including *Acta Crystallographica*, decided against publishing long tables of tensor components, six per atom, and started to classify them as Supplementary Material, to be filed away in the vaults of libraries and similar depositories.

(6) See, for example, B. T. M. Willis and A. W. Pryor, "Thermal Vibrations in Crystallography", Cambridge University Press, Cambridge, England, 1975.

(7) For a molecule consisting of  $N$  atoms, there are  $3N - 6$  independent structural parameters, but it is often possible to reduce the dimensionality of the problem drastically by ignoring parameters or linear combinations of parameters that stay more or less constant along the reaction path. Factor analysis may be useful for deciding how many dimensions are relevant for any given problem.<sup>8</sup>

(8) P. Murray-Rust and R. Bland, *Acta Crystallogr., Sect. B*, **B34**, 2527 (1978).

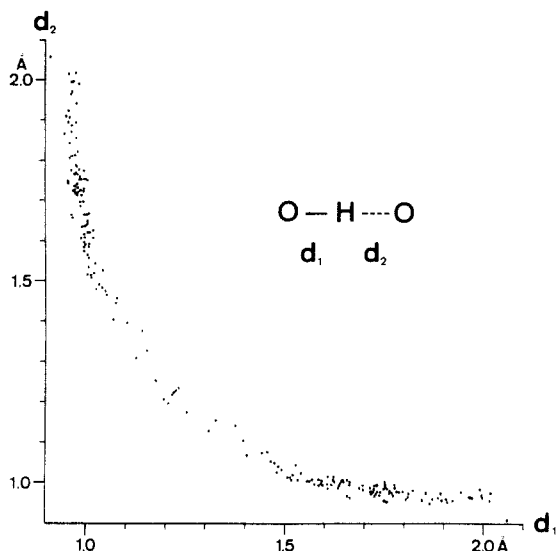


Figure 1. Distribution of HO(1) distances  $d_1$  vs.  $d_2$  in O-H...O hydrogen bonds with OH angle  $>170^\circ$  (adapted from ref 11).

representation is that it affords an immediate connection with the concept of the molecular potential energy hypersurface, a concept almost indispensable to any modern discussion of chemical reaction dynamics.<sup>9</sup> Very briefly, each point of the many-dimensional parameter space is associated with a potential energy  $V$ ; the minima of  $V$  correspond to stable chemical species, the passes to transition states, and the curves following the energy valleys and connecting minima via the lowest passes between them to deformation of the fragment along chemical reaction paths. The problem of how to construct the molecular energy hypersurface from experimental data or from theoretical calculations is a formidable one that we do not have space to discuss here.<sup>10</sup>

The basic assumption behind the structure-correlation method is that a distribution of sample points corresponding to *observed* structures will tend to be concentrated in low-lying regions of the potential energy surface. This is really equivalent to the assumption that the interaction energy between the molecule or molecular fragment of interest and its various crystal or molecular environments can be regarded as a small perturbation relative to the total molecular potential energy.

There are thus two quite distinct ways of progressing from the static to the dynamic interpretation of crystal structure results. One way is to exploit the information about mean-square vibration amplitudes of motion from one or a few accurately determined structures. The other is to look for correlations among the relevant structural parameters from many structures.

### The Structure-Correlation Method in Action

We begin by discussing a number of ligand-exchange reactions  $L-A + L' \rightarrow L + A-L'$ . Whatever the detailed mechanism, it is clear that this kind of reaction involves breaking an A-L bond, i.e., lengthening an A-L distance from a value typical of a bond to a value typical of a van der Waals distance. It also involves forming a new

(9) For example, R. D. Levine and R. B. Bernstein, "Molecular Reaction Dynamics", Oxford University Press, New York, 1974.

(10) K. Müller, *Angew. Chem.*, **92**, 1 (1980); *Angew. Chem. Int., Ed. Engl.*, **19**, 1 (1980).

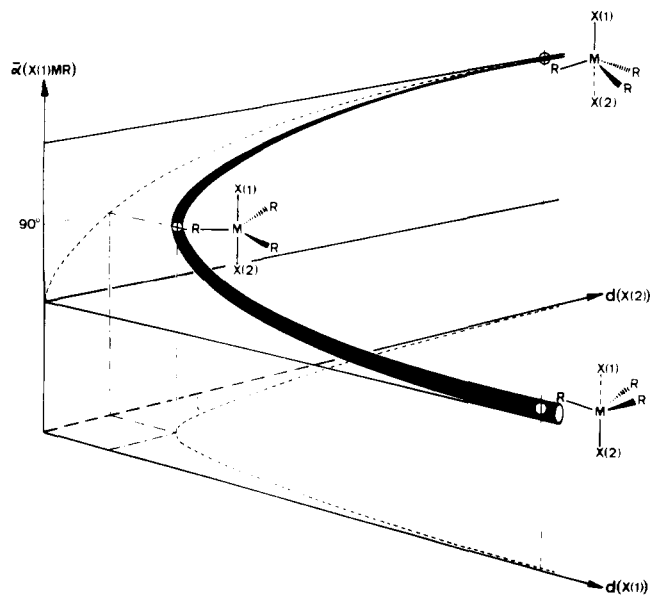


**Figure 2.** Schematic representation of reaction path for an  $S_N2$ -like process in the three-dimensional parameter space spanned by the two X-M distances and an X-M-R angle.

A-L' bond, i.e., shortening a van der Waals (or larger) distance to a bond distance. Such changes are of the order of 1–2 Å. Neutron-diffraction studies of collinear or nearly collinear O-H...O hydrogen bonds show that the OH distances cover the range from 0.9 to >2 Å almost continuously.<sup>11</sup> Figure 1 shows the distribution of sample points for the two OH distances in each bond, which are obviously strongly correlated. The distribution outlines a quite well-defined path in the two-dimensional parameter space. It is this path that we interpret as the reaction path for a proton-transfer reaction. The reaction may be classified as an associative ligand exchange at the proton since it goes through an intermediate point where the proton has two ligands symmetrically bonded to it. The thinning-out of the density in this region suggests that the potential energy varies along the path and is highest close to the symmetrical structure.<sup>12</sup>

Very similar distributions are obtained for opposite bond distances in other three-center-four-electron systems X-M...Y where X, Y, are Lewis bases (nucleophilic centers) and M is a Lewis acid (electrophilic center). The examples include not only linear triatomics, such as  $I_3^-$  and S-S...S in thiathiophthenes,<sup>13</sup> but also five-coordinate species of the type X-MR<sub>3</sub>...Y with M = Cd<sup>II</sup><sup>14</sup> and Sn<sup>IV</sup><sup>15</sup> as electrophilic centers with miscellaneous nucleophiles X and Y.<sup>16</sup> To describe the continuous transition of the five-coordinated species from monocapped tetrahedra to trigonal bipyramids at least one additional structural parameter has to be

considered; the parameter space is then at least three dimensional. This additional parameter is conveniently chosen as the average X-M-R angle, which shows a continuous change from a value greater than 90° to one smaller than 90° as the X-M bond is broken and the M-Y bond is formed (Figure 2). The experimental sample points for these associative ligand-exchange reactions describe the kind of process that has long been postulated to occur during Walden inversion ( $S_N2$  displacement with inversion of configuration). Similar results are obtained from calculations with various quantum-chemical models.<sup>10</sup>

A study of SnR<sub>2</sub>X<sub>2</sub> crystal structures (X = electronegative ligand) reveals that most contain six-coordinate species covering the range between bicapped tetrahedra and distorted octahedra with transoid R groups.<sup>15</sup> These species map the path for the double displacement reaction  $SnR_2X_2 + 2Y \rightarrow [SnR_2X_2Y_2] \rightarrow SnR_2Y_2 + 2X$ , where the two incoming nucleophilic centers Y approach the central Sn atom approximately opposite the two breaking Sn-X bonds. Although there is no kinetic or mechanistic analogy for this termolecular ( $S_N3$ ) process, the distribution of sample points in the three-dimensional space spanned by  $\Delta d_x$ ,  $\Delta d_y$ , and average X-Sn-R angle, is very similar to that found for the  $S_N2$ -like reaction path.<sup>17</sup>

The distribution of distances and angles is not always as uniform, nor does it always extend over such a large range as in the above examples. Nucleophiles approach the S atoms of organic sulfides and sulfonium ions preferentially in directions trans to existing bonds;<sup>18,19</sup> the Nu...S distances may be significantly less than the sum of the van der Waals radii, but they are not short enough to cause a perceptible lengthening of the opposite bond. Such directed nonbonded contacts have been termed secondary bonds<sup>20</sup> and may often be interpreted as structural expressions of "incipient stages of chemical reactions".<sup>21</sup>

In most of the examples discussed so far the fragments of interest have been embedded in different crystal structures. It is also possible to vary the position and relative orientation of mutually complementary reactive groups by embedding these in molecules of appropriately chosen structures. Medium rings with electrophiles and nucleophiles in transannular relationship (1) are good examples;<sup>22</sup> e.g., compound 2 shows solvent-dependent C-O stretching frequencies<sup>23</sup> and <sup>13</sup>C chemical shifts<sup>24</sup> that have been explained in terms of a "transannular interaction". The relative arrangement of the amino and carbonyl groups can be modified by embedding them in different molecular skeletons, as in 3 or 4. Molecules of types 1–4 show N...C=O distances ranging from ~3 Å to ~1.5 Å and carbonyl groups that deviate markedly from the usual

(11) See, for example, P. Schuster, G. Zundel, and C. Sandorfy, Eds., "The Hydrogen Bond", Vol. 2, North Holland, Amsterdam, 1976, Chapter 8.

(12) Note, however, that ab initio calculations on [HOHOH]<sup>-</sup> and [H<sub>2</sub>O-H-OH<sub>2</sub>] show energy minima rather than maxima at the symmetrical structures: B. O. Roos, W. P. Kraemer, and G. H. F. Diercksen, *Theor. Chim. Acta*, **42**, 77 (1976); P. J. Desmeules and L. C. Allen, *J. Chem. Phys.*, **72**, 4731 (1980).

(13) H. B. Bürgi, *Angew. Chem.*, **87**, 461 (1975); *Angew. Chem., Int. Ed. Engl.*, **14**, 460 (1975).

(14) H. B. Bürgi, *Inorg. Chem.*, **12**, 2321 (1973).

(15) D. Britton and J. D. Dunitz, *J. Am. Chem. Soc.*, **103**, 2971 (1981).

(16) When X and Y are different, we plot  $\Delta d_x$  against  $\Delta d_y$ , where  $\Delta d$  is the difference between the observed distance and the corresponding standard single-bond distance.

(17) Termolecular processes of this type are obviously disfavored entropically and have been largely ignored in discussions of chemical reactivity. Might they be of importance in enzymatic reactions where entropic effects are presumably not so crucial as in solution reactions?

(18) R. E. Rosenfield, R. Parthasarathy, and J. D. Dunitz, *J. Am. Chem. Soc.*, **99**, 4860 (1977).

(19) D. Britton and J. D. Dunitz, *Helv. Chim. Acta*, **63**, 1068 (1980).

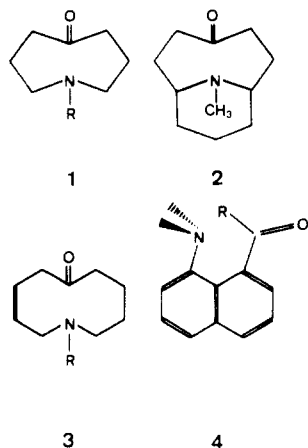
(20) N. W. Alcock, *Adv. Inorg. Radiochem.*, **15**, 1 (1972).

(21) H. B. Bürgi, J. D. Dunitz, and E. Shefter, *Acta Crystallogr., Sect. B*, **B30**, 1517 (1974).

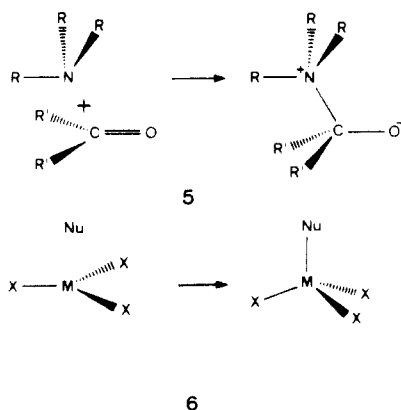
(22) N. J. Leonard, *Acc. Chem. Res.*, **12**, 423 (1979).

(23) N. J. Leonard, private communication; G. I. Birnbaum, *J. Am. Chem. Soc.*, **96**, 6165 (1974).

(24) T. T. Nakashima and G. E. Macial, *Org. Magn. Reson.*, **4**, 321 (1972).



coplanar geometry, a decrease in  $N\cdots C=O$  distance being accompanied by an increase in nonplanarity at carbonyl carbon and a slight lengthening of the  $C=O$  distance.<sup>25,26</sup> Furthermore, the approach direction of the nucleophile is not perpendicular to the  $C=O$  bond but at an angle of about  $105^\circ$ , as is evident from Figure 3. The implications for the mechanism of addition of amino N to carbonyl C (5) and related reactions have



been discussed by several authors.<sup>25,27</sup>

Lewis acids other than  $R_2C=O$  are expected to show similar behavior. Examples include addition of a nucleophile Nu to planar  $MX_3$  molecules (6) such as  $AlCl_3$ ,  $PO_3^-$ ,  $SO_3$ , and  $SnCl_3^+$ . The threefold symmetry in these species reduces the number of independent parameters to three: the Nu-M distance  $r_1$ , the M-X distance  $r_2$ , and the Nu-M-X angle  $\theta_{12}$ , an alternative measure of the nonplanarity of  $MX_3$ . It is found<sup>28</sup> that decrease of  $r_1$  is associated with increase in  $r_2$  and  $\theta_{12}$ , as expected by analogy to the carbonyl example. Results obtained for  $AlCl_4^-$ ,  $PO_4^{3-}$ , and  $SO_4^{2-}$  structural fragments have been combined in Figure 4 because the correlation functions are quantitatively indistinguish-

(25) H. B. Bürgi, J. D. Dunitz, and E. Shefter, *J. Am. Chem. Soc.*, **95**, 5065 (1973).

(26) (a) G. I. Birnbaum, *J. Am. Chem. Soc.*, **96**, 6165 (1974). (b) M. Kaftory and J. D. Dunitz, *Acta Crystallogr., Sect. B*, **B31**, 2912, 2914 (1975); **B32**, 1 (1976). (c) E. Bye and J. D. Dunitz, *ibid.*, **B34**, 3245 (1978). (d) W. B. Schweizer, ETH Dissertation, No. 5948, 1977. (e) W. B. Schweizer, G. Procter, M. Kaftory, and J. D. Dunitz, *Helv. Chim. Acta*, **61**, 2783 (1978).

(27) For example: (a) H. B. Bürgi, J. D. Dunitz, J. M. Lehn, and G. Wipff, *Tetrahedron*, **30**, 1563 (1974). (b) J. E. Baldwin, *J. Chem. Soc., Chem. Commun.*, 738 (1976). (c) N. T. Anh and O. Eisenstein, *Nouv. J. Chim.*, **1**, 61 (1977). (d) R. E. Rosenfield and J. D. Dunitz, *Helv. Chim. Acta*, **61**, 2176 (1978). (e) M. M. Kayser and P. Morand, *Tetrahedron Lett.*, 695 (1979).

(28) P. Murray-Rust, H. B. Bürgi, and J. D. Dunitz, *J. Am. Chem. Soc.*, **97**, 921 (1975); *Acta Crystallogr., Sect. B*, **B34**, 1793 (1978).

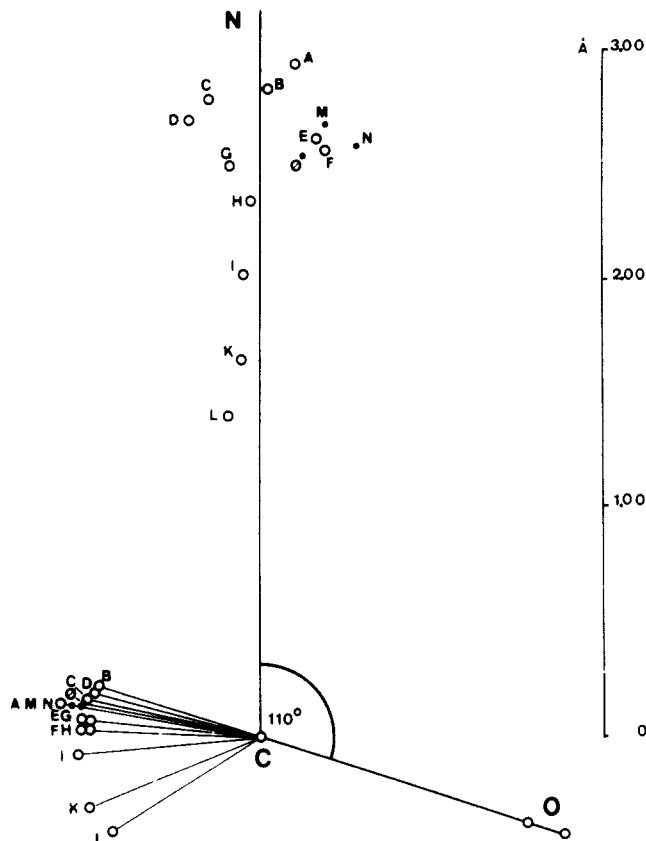


Figure 3. Relative positions of N, C, and O atoms and of the RCR' plane in 14 molecules of types 1-4 showing  $N\cdots C=O$  interactions, taken from ref 26d.

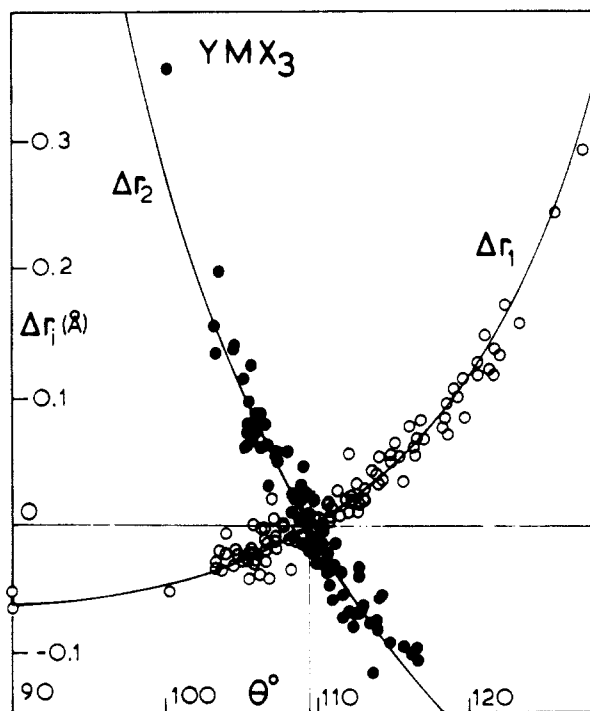


Figure 4. Correlation plots for  $SO_4^{2-}$ ,  $PO_4^{3-}$ , and  $AlCl_4^-$  tetrahedra referred to a common origin (reproduced with permission from ref 28). See text for explanation of symbols.

able for these three species.

### Isomerization Reaction Paths

The structure-correlation method has been applied to map reaction paths for several types of isomerization

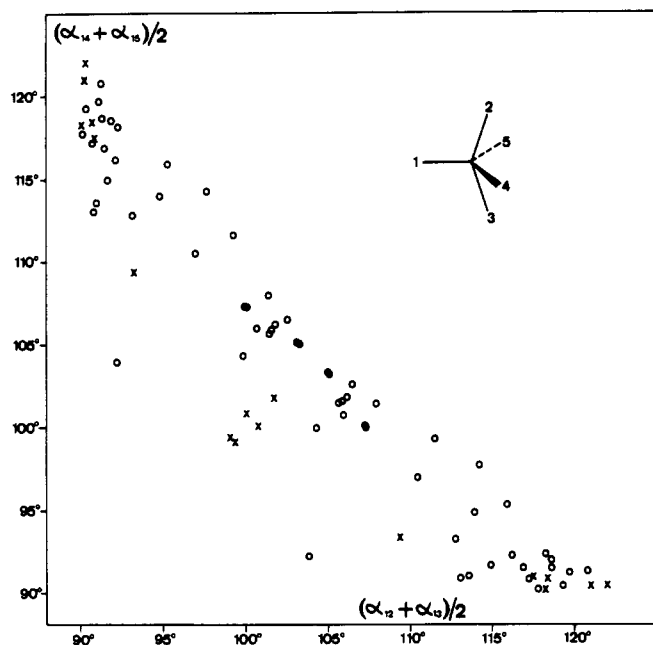
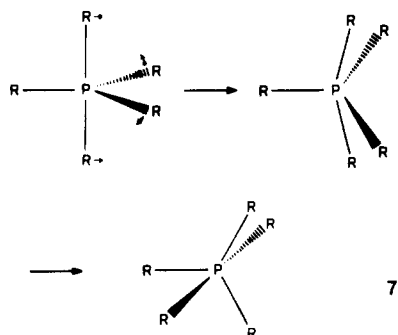


Figure 5. Distribution of  $(\alpha_{12} + \alpha_{13})/2$  vs.  $(\alpha_{14} + \alpha_{15})/2$  angles for five-coordinate phosphorus compounds with carbon or oxygen ligands (O) and for  $d^8$ -metal complexes with five equal ligands (X).<sup>31</sup>

process. One of the first applications<sup>29</sup> was to the Berry process (7), which explains the NMR spectroscopic



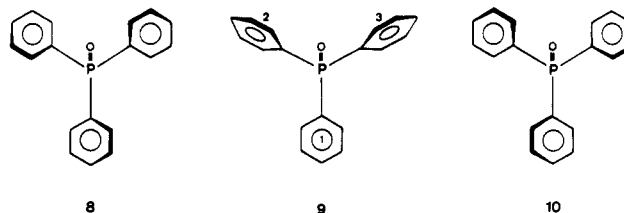
equivalence of the fluorine atoms in  $PF_5$ . More recently, the correlation of bond-angle changes implied in 7 has been mapped from data obtained by systematic structure analyses of a large variety of five-coordinate phosphorus compounds.<sup>30</sup> Figure 5 shows a scatter plot based on a somewhat different selection of data.<sup>31</sup> It suggests that in trigonal-bipyramidal phosphorus compounds, opening of an equatorial angle is associated with an approximately equal degree of closing of the axial angle; for  $d^8$ -metal complexes, opening of the equatorial angle seems to run ahead of the closing of the axial angle in the first half of the reaction path and to lag behind in the second half. The difference between the two families is most apparent near the midpoint (quadrilateral pyramid), with angles of about  $152^\circ$  for phosphorus and of about  $162^\circ$  for the metals. The possibility of distinguishing between these values depends on the broadness of the distribution of sample points normal to the reaction path.

(29) E. L. Muetterties and L. J. Guggenberger, *J. Am. Chem. Soc.*, **96**, 1748 (1974).

(30) For a review see R. R. Holmes, *Acc. Chem. Res.*, **12**, 257 (1979).

(31) Figure 6 is based on our own compilation of structures in version 1982.1 of the Cambridge Structural Database; included are data for 31 five-coordinate phosphorus compounds with C or O ligands and nine  $d^8$ -metal complexes with five chemically equivalent ligands.

The stereoisomerization of triphenylphosphine oxide is an example of a conformational interconversion for which a fairly detailed reaction path has been derived.<sup>32</sup> In the solid state the molecule occurs as a chiral propeller with approximate  $C_3$  symmetry (8). The main

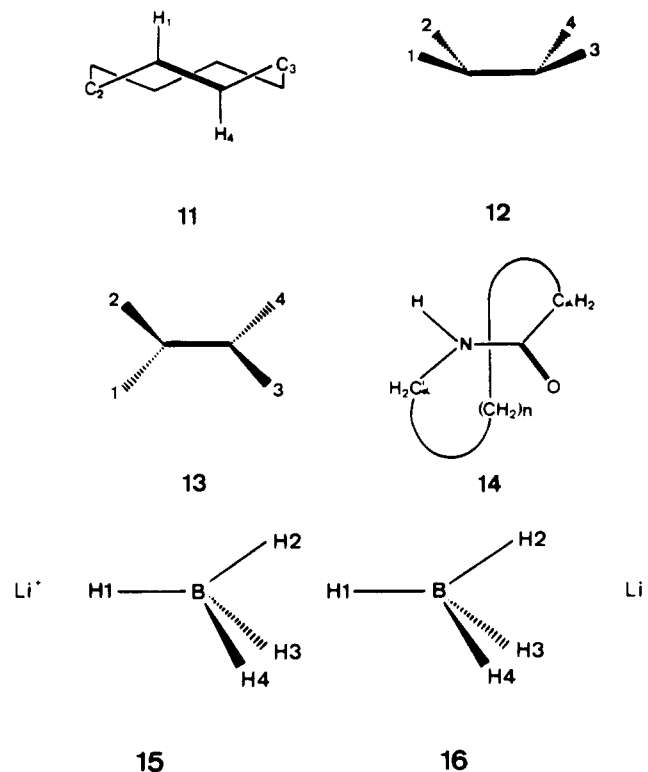


deformations observed in a variety of complexes correspond to what has been described as a two-ring flip mechanism.<sup>33</sup> These deformations take one phenyl ring into a horizontal conformation and the other two into positions about  $10^\circ$  short of being perpendicular and about  $10^\circ$  beyond to give the mirror-symmetric structure 9. Further rotation of the phenyl rings leads to a propeller of opposite chirality (10). The two parts of the path leading from 8 to 9 and from 9 to 10 are symmetry related in the space of the three torsion angles. By symmetry, structure 9 must correspond to an energy minimum (reaction intermediate) or an energy maximum (transition state) along this path.

### Interpretation of Mean-Square Vibration Amplitudes

Atomic mean-square vibration amplitudes determined by X-ray or neutron diffraction include the effect

Chart I



(32) E. Bye, W. B. Schweizer, and J. D. Dunitz, *J. Am. Chem. Soc.*, **104**, 5893 (1982).

(33) See K. Mislow, *Acc. Chem. Res.*, **9**, 26 (1976), for a review of experimental work and force-field calculations leading to this type of mechanism for the stereoisomerization of structurally related molecules in solution.

Table I  
Mean-Square Atomic Displacement  $U$  of M and N Along  
the MN Bond with Distance  $d(\text{MN})$  in  $\text{M}(\text{NO}_2)_6^{4-}$ <sup>a</sup>

	$\text{Cu}(\text{NO}_2)_6^{4-}$	$\text{Ni}(\text{NO}_2)_6^{4-}$
$U(\text{N})$	0.0380 (20) Å <sup>2</sup>	0.0132 (9) Å <sup>2</sup>
$U(\text{M})$	0.0172 (1) Å <sup>2</sup>	0.0110 (1) Å <sup>2</sup>
$\Delta U$	0.0208 (20) Å <sup>2</sup>	0.0022 (10) Å <sup>2</sup>
$d(\text{MN})$	2.111 (4) Å	2.080 (2) Å

<sup>a</sup> From ref 38 and 39.

of all motions in the crystal; rotational and translational vibrations of molecules and internal molecular motions, as well as the effect of static disorder, i.e., random distribution of atoms among two or more sites.<sup>34</sup> Each type of motion will introduce certain kinds of correlation among the  $U^{ij}$  components of different atoms, and it is by analyzing these correlations that we may hope to derive information about the importance of different types of motion.

The simplest case is that of a perfectly rigid molecule, which can perform only translational and librational oscillations around its equilibrium position and orientation. For each type of motion the displacements of all atoms are exactly in phase, and, in particular, the mean-square displacements of any pair of atoms are exactly equal along the line connecting them. The amplitudes of such rigid-body motions may be extracted from the vibrational parameters  $U^{ij}$  of the atoms.<sup>35</sup> Of course, many molecules are quite unrigid,<sup>36</sup> but the mean-square displacements of pairs of bonded atoms are usually equal along the bond direction<sup>37</sup> within experimental accuracy. If they are not, there must be a relative motion of the atoms in that direction.

A good example is provided by a comparison of the  $\text{Ni}(\text{NO}_2)_6^{4-}$  and  $\text{Cu}(\text{NO}_2)_6^{4-}$  anions in the  $\text{K}_2\text{PbM}(\text{NO}_2)_6$  structure;<sup>38,39</sup> both anions have  $T_h(m3)$  site symmetry, and the mean-square displacements of the N and M atoms along the six equivalent M–N bond directions are given in Table I. They are nearly equal for Ni and N, as expected for an octahedral  $d^8$  complex, but significantly different for Cu and N. For  $\text{Cu}^{2+}$  with its  $d^9$  electron configuration, Jahn–Teller theory predicts a distorted octahedral coordination with two longer bonds and four shorter ones. Three such elongated tetragonal bipyramids are possible and may interconvert by way of compressed tetragonal bipyramids (Figure 6a) in a dynamic pseudorotation process, where the bond lengths are given by  $d_1 = \bar{d} + 2\Delta \cos \varphi$ ,  $d_2 = \bar{d} + 2\Delta \cos(\varphi + (2\pi/3))$ , and  $d_3 = \bar{d} + 2\Delta \cos(\varphi - (2\pi/3))$  (Figure 6b). For this process  $\bar{d}_1 = \bar{d}_2 = \bar{d}_3 = \bar{d}$ , and the mean-square deviation from  $\bar{d}$  is  $2\Delta^2$ . This may be identified

(34) From diffraction measurements at a single temperature, it is difficult to distinguish between the effects of dynamic disorder, i.e., vibrations, and static disorder.

(35) D. W. J. Cruickshank, *Acta Crystallogr.*, **9**, 757 (1956); V. Schomaker and K. N. Trueblood, *Acta Crystallogr., Sect. B*, **B24**, 63 (1968).

(36) According to a recent study (K. N. Trueblood and J. D. Dunitz, *Acta Crystallogr., Sect. B*, **B39**, 120 (1983) force constants, frequencies, and rotation barriers for certain types of internal molecular motion can be estimated from atomic vibrational amplitudes in crystals and are often in reasonable agreement with values obtained by other methods. See also ref 41. For a simple test of molecular rigidity from atomic vibration tensors see R. E. Rosenfield, K. N. Trueblood, and J. D. Dunitz, *Acta Crystallogr., Sect. A*, **A34**, 828 (1978).

(37) F. L. Hirshfield, *Acta Crystallogr., Sect. A*, **A32**, 239 (1976).

(38) D. L. Cullen and E. C. Lingafelter, *Inorg. Chem.*, **10**, 1264 (1971); N. W. Isaacs and C. H. L. Kennard, *J. Chem. Soc. A*, 386 (1969).

(39) S. Takagi, M. D. Joesten, and P. G. Lenhert, *Acta Crystallogr., Sect. B*, **B31**, 1968 (1975).

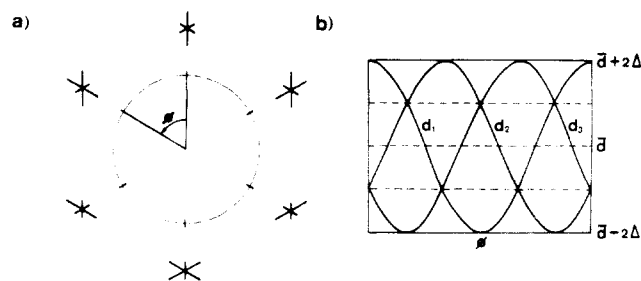


Figure 6. (a) Pseudorotation path for a dynamic Jahn–Teller distortion from perfect octahedral symmetry. The total amount of distortion,  $2[(d_1 - d_0)^2 + (d_2 - d_0)^2 + (d_3 - d_0)^2]$ , is constant along the path. (b) Variation of  $d_1, d_2, d_3$  along the pseudorotation path.

with  $\Delta U$ ,<sup>40</sup> the extra motion of the N atom relative to Cu (Table I), to yield an experimental measure of  $\Delta$  and hence of the instantaneous structure of a compressed or elongated octahedron;<sup>41</sup> for  $\varphi = 0$ , we obtain  $d_1 = 2.315$  Å and  $d_2 = d_3 = 2.009$  Å. On cooling, some compounds in the  $\text{K}_2\text{MCu}(\text{NO}_2)_6$  family undergo a transition to a low-temperature phase containing elongated  $\text{Cu}(\text{NO}_2)_6^{4-}$  octahedra with  $D_{2h}(mmm)$  site symmetry. The average Cu–N bond lengths observed in this low-temperature phase with M = Ca, Sr, Ba<sup>42</sup> are  $d_1 = 2.31$  Å,  $d_2 \sim d_3 = 2.04$  Å, in good agreement with the values derived from the  $\Delta U$  values for the dynamical process. Analogous results have been obtained for  $\text{Cu}^{2+}$  coordinated to six chemically equivalent amino groups,<sup>41</sup> hydroxyl groups, water molecules, and other oxygen-containing ligands,<sup>43</sup> as well as for  $\text{Mn}^{3+}$  coordinated to six fluoride ions.<sup>44</sup>

### Ground-State Structure and Reactivity

There are a few examples where displacements from standard bond lengths and angles along a reaction path can be not only discerned but also correlated with the actual kinetic behavior of molecules in a chemical reaction. In solution the keto acid 17 and its hydroxy lactone isomer 18 coexist as a rapidly interconverting equilibrium mixture with an activation enthalpy of about 6 kcal mol<sup>-1</sup> estimated by line-shape analysis of <sup>13</sup>C NMR signals.<sup>45</sup> The hydroxy and methoxy lactones show a pattern of bond-length and -angle deformations corresponding to an initial stage of the ring-opening reaction. Similarly, on the ring-opened side, the keto acid and keto methyl ester show structural features corresponding to displacement along the reverse, ring-closure path. Even the hydrogen-bonding patterns found in the crystals correspond to incipient stages of the proton-transfer processes that accompany ring opening and closure. Barriers for the pericyclic ring-closure reaction type 19 → 20 are also typically quite small, and analogous displacements along the reaction coordinate are found for this reaction.<sup>46</sup>

(40) The evidence that  $\Delta U$  is in this case due to dynamic and not to static disorder comes from nondiffraction methods, mainly ESR.<sup>41</sup>

(41) J. H. Ammeter, H. B. Bürgi, E. Gamp, V. Meyer-Sandrin, and W. P. Jensen, *Inorg. Chem.*, **18**, 733 (1979).

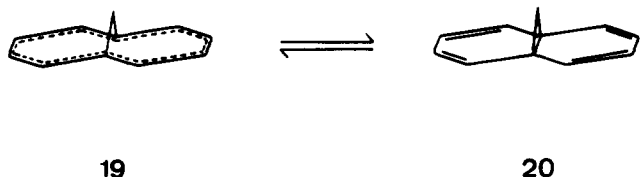
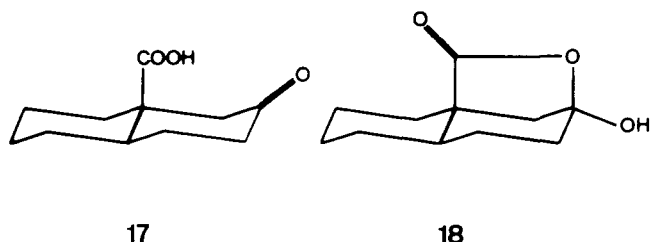
(42) S. Takagi, P. G. Lenhert, and M. D. Joesten, *J. Am. Chem. Soc.*, **96**, 6606 (1974); S. Takagi, M. Joesten, and P. G. Lenhert, *Acta Crystallogr., Sect. B*, **B32**, 2524 (1976); S. Takagi, M. D. Joesten, and P. G. Lenhert, *Acta Crystallogr., Sect. B*, **B31**, 596 (1975).

(43) E. Gamp, ETH Dissertation, No. 6673, 1980.

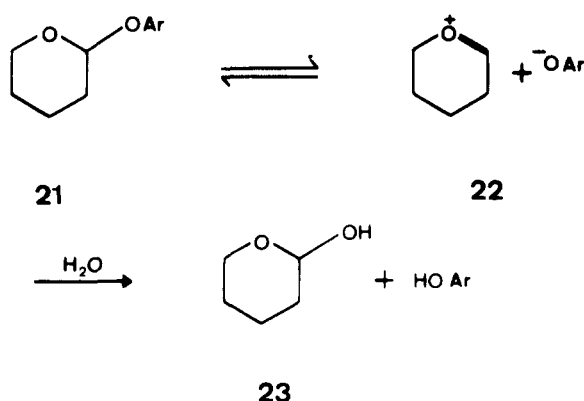
(44) A. Vedani, Thesis, University of Zürich, 1981.

(45) D. J. Chadwick and J. D. Dunitz, *J. Chem. Soc., Perkin Trans. 2*, 276 (1979).

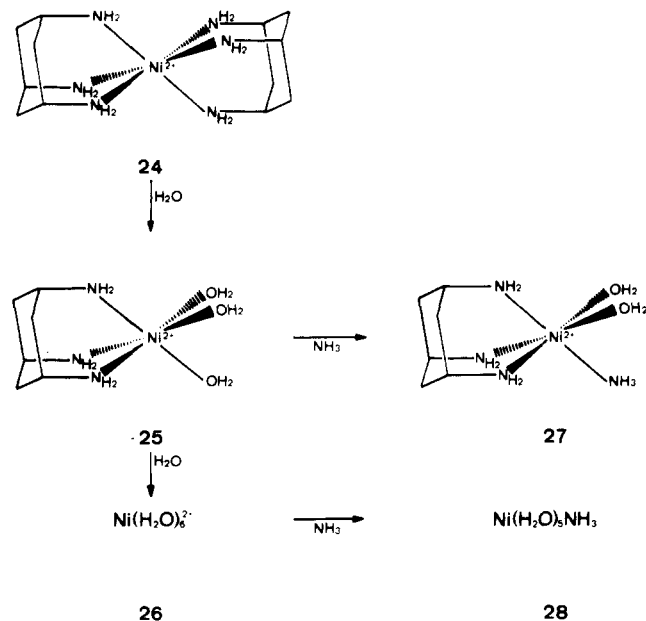
(46) H. B. Bürgi, E. Shefter, and J. D. Dunitz, *Tetrahedron*, **31**, 3089 (1975).



Crystal structures of alkyl aryl acetals 21 show displacements along the reaction path<sup>47</sup> for the hydrolysis reaction 21  $\rightarrow$  23 when the exocyclic bond is axial but



not when it is equatorial.<sup>48</sup> For this series, the bond-length changes can be correlated with the activation energies for the spontaneous hydrolysis: an increase of 0.01 Å in the length of the exocyclic bond is equivalent to a decrease of about 3 kcal mol<sup>-1</sup> in the activation energy! Similarly, for the hydrolysis 24  $\rightarrow$  25  $\rightarrow$  26 the



(47) P. G. Jones and A. J. Kirby, *J. Chem. Soc., Chem. Commun.*, 288 (1979).

(48) An example of the expression of stereoelectronic factors in the ground states of molecules. For chemically equivalent but conformationally different C-O bonds the stereoelectronic effect alone results in a bond-length difference of about 0.025 Å.<sup>49</sup>

longer Ni-N bonds in 24 (2.133 Å) are broken about 10<sup>2</sup> times faster than the shorter Ni-N bonds in 25 (2.070 Å), and for the ammonolysis reactions 25  $\rightarrow$  27 and 26  $\rightarrow$  28 the longer Ni-O bonds in 25 (2.10 Å) are broken about 10<sup>2</sup> times faster than the shorter Ni-O bonds in 26 (2.05 Å).<sup>50</sup> For these reactions, it would appear that differences in the transition state are unimportant compared to differences in ground-state structure.

A still more persuasive example comes from a study of symmetric electron-transfer processes,<sup>51</sup>  $\text{ML}_6^{2+} + \text{ML}_6^{3+} \rightarrow \text{ML}_6^{3+} + \text{ML}_6^{2+}$ . In order to reach the transition state the larger  $\text{ML}_6^{2+}$  must contract and the smaller  $\text{ML}_6^{3+}$  must expand until both complexes are of equal size. The activation energy can be approximated by  $3\bar{f}(\Delta r)^2/2$ , where  $\bar{f}$  is the mean of the symmetric stretching force constants in  $\text{ML}_6^{2+}$  and  $\text{ML}_6^{3+}$  and  $\Delta r$  is the difference in equilibrium bond length. Such differences are available for  $\text{Fe}(\text{H}_2\text{O})_6^{2+/3+}$  (0.14 Å),  $\text{Ru}(\text{H}_2\text{O})_6^{2+/3+}$  (0.09 Å), and  $\text{Ru}(\text{NH}_3)_6^{2+/3+}$  (0.04 Å). The rate constants reflect the structural differences, the reaction of  $\text{Ru}(\text{NH}_3)_6^{2+/3+}$ , which is closest to the transition state, being about 10<sup>3</sup> times faster than that for  $\text{Fe}(\text{H}_2\text{O})_6^{2+/3+}$  with  $\text{Ru}(\text{H}_2\text{O})_6^{2+/3+}$  intermediate.

The systematic correlation of accurate structural data with reaction rates is only in its beginning, but it may well develop into another area of chemistry where crystallography can make essential contributions.

#### How Flat Was My Valley?

It seems tempting to give quantitative expression to the notion that sample points tend to congregate in low-lying regions of the potential energy surface by fitting the density of points to some function like  $\exp(-\alpha E)$ . One might even be enticed to set  $\alpha = 1/(kT)$  in imitation of the Boltzmann distribution. Although such ideas have undeniable attraction, there are several difficulties. The value of  $\alpha$  can be expected to depend on the nature of the fragment and the type of environment (ionic, molecular, etc.) in which it is embedded. At present we have no way of estimating this quantity. Even if we had, any values of  $E$  obtained in this way would have to be apportioned partly to deformation of the fragment and partly to the perturbation due to the environment. Perhaps the best we can hope for are relative magnitudes of potential constants such as those contained in eq 2. We are not aware of a study where such ratios have been determined from analyses of scatter plots and compared with values obtained from other sources.<sup>52</sup>

#### Minimum-Energy Paths or Response Paths?

Generally, it is difficult to decide between two possible interpretations of the observed correlations: as minimum-energy paths or as response paths. We shall discuss both possibilities.

As a first example we consider the trans-cis isomerization of a C=C double bond and suppose we trap

(49) K. L. Brown, G. J. Down, J. D. Dunitz, and P. Seiler, *Acta Crystallogr., Sect. B*, **B38**, 1241 (1982).

(50) G. Schwarzenbach, H. B. Bürgi, W. P. Jensen, G. A. Lawrence, L. Mønsted, and A. M. Sargeson, *Inorg. Chem.*, submitted for publication.

(51) P. Bernhard, H. B. Bürgi, J. Hauser, H. Lehmann, and A. Ludi, *Inorg. Chem.*, **21**, 3936 (1982); N. Sutin in "Tunneling in Biological Systems", B. Chance, et al., Eds., Academic Press, New York, 1979, p 201.

(52) Qualitative comparisons of experimental distributions with Boltzmann distributions based on empirical force fields have been made for structural parameters of hydrogen-bonded systems.<sup>53</sup>



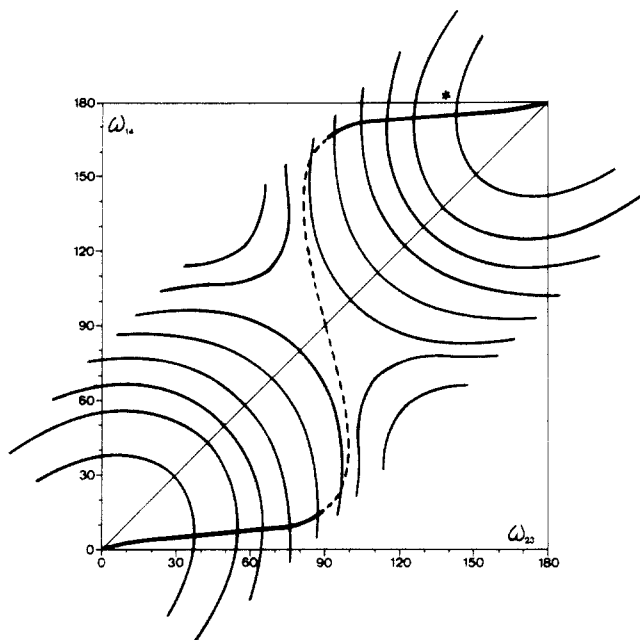


**Figure 7.** Two-dimensional energy surface for trans-cis isomerization of a C=C double bond, preserving  $C_2$  symmetry, calculated from data by Ermer.<sup>54</sup> Contours at energy intervals of 10 kcal mol<sup>-1</sup>. Also shown are the minimum energy path (along the positive diagonal) and the conditional minimum energy path or constraint path with  $\omega_{23}$  as constraint coordinate. The star represents values of  $\omega_{14}$  and  $\omega_{23}$  found in *trans*-cyclooctene.

intermediate conformations by inserting the double bond in a medium ring, as in *trans*-cyclooctene (11) (see Chart I). In the strained cycloolefin atoms 2 and 3 are forced out of the plane of the double bond, which loses its inversion center but retains  $C_2$  symmetry. The potential function derived by Ermer<sup>54</sup> for symmetric (with respect to  $C_2$ ) out-of-plane deformation of strained olefins may be written in terms of torsion angles  $\omega$  (in deg,  $V$  in kcal mol<sup>-1</sup>):

$$V = 5.55(\omega_{14} - \omega_{23})^2 + 31.5 \{1 - \cos(\omega_{14} + \omega_{23})\} - 3.5 \{1 - \cos 2(\omega_{14} + \omega_{23})\} = k\chi^2/2 + V_2(1 - \cos \tau)/2 + V_4(1 - \cos 2\tau)/2 \quad (1)$$

The first term in (1) represents the strain energy for out-of-plane bending of the two carbon atoms ( $\chi$ , 12), and the second and third terms represent the strain energy of torsional deformation ( $\tau$ , 13). In a medium ring  $\omega_{23}$  is more or less fixed by ring-closure conditions, so in any given ring  $\omega_{14}$  is practically forced to take a value which minimizes  $V$  for a particular value of  $\omega_{23}$ :

$$dV/d\omega_{14} = 0 = k\chi + V_2 \sin \tau + 2V_4 \sin 2\tau \quad (2)$$

The resulting relationship between  $\omega_{23}$  and  $\omega_{14}$ , shown in Figure 7, can be described as a conditional minimum energy path or constraint path. It is quite different from the minimum energy path ( $\omega_{23} = \omega_{14}$ ) for trans-cis isomerization. The experimental point for *trans*-cyclooctene<sup>55</sup> lies close to the constraint path. Conversely, from experimental values of out-of-plane deformation parameters approximate relationships may be derived between the potential constants describing energy

(53) R. Taylor, *J. Mol. Struct.*, **73**, 125 (1981).

(54) O. Ermer, "Aspekte von Kraftfeldrechnungen", Wolfgang Baur Verlag, Munich, 1981, Chapter 4.

(55) M. Traetteberg, *Acta Chem. Scand., Ser. B*, **B29**, 29 (1975).

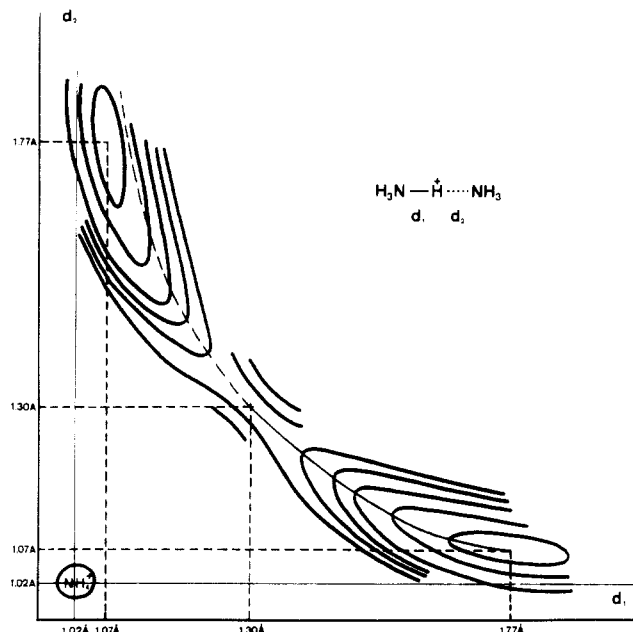


**Figure 8.** Two-dimensional energy surface for the proton-transfer reaction in  $[H_3NH...NH_3]^+$  (adapted from ref 60).

surfaces. This has been done in a qualitative way for the amide group by studying the out-of-plane deformations in a series of medium-ring lactams,<sup>56</sup> here the ring torsion angle  $\omega(C_\alpha CNC'_\alpha)$  is constrained (14) and its value was found to be coupled with out-of-plane bending at the N atom.<sup>57</sup> The ring torsion angles in the lactams are almost the same as those in the corresponding cycloolefins, illustrating that they are determined mainly by geometry and do not depend much on the energy functions.

A characteristic feature of the two-dimensional energy function shown in Figure 7 is that the contours round the minimum are not too far from circles. If  $k$  were much larger the contours would be more elliptical and the constraint path (following the tangents parallel to  $\omega_{14}$ ) would lie closer to the minimum energy path  $\omega_{23} = \omega_{14}$ . A calculated energy surface for proton transfer in  $H_3NH...NH_3^+$  (Figure 8) shows an example of a very narrow reaction channel.<sup>60</sup> Whatever the constraint on such a system, the conditional minimum in energy cannot deviate far from the minimum energy path. The reaction channel of Figure 8 agrees in its narrowness and general shape with the experimental distribution for OH...O hydrogen bonds shown in Figure 1.

The identification of the constraint coordinate is not always straightforward, nor indeed is the concept always a useful one. For example, the tetrahedral fragments  $PO_4^{3-}$  and  $SO_4^{2-}$  discussed earlier<sup>28</sup> occur in a variety of environments: cations in different positions, protons or hydrocarbon groups attached to the O atoms, etc. The distortions from tetrahedral symmetry follow a

(56) F. K. Winkler and J. D. Dunitz, *J. Mol. Biol.*, **59**, 169 (1971); J. D. Dunitz and F. K. Winkler, *Acta Crystallogr., Sect. B*, **B31**, 251 (1975).

(57) Similar couplings between different types of out-of-plane deformations have also been observed for the enamine group with various substituents,<sup>58</sup> and for cyclophanes and annulenes.<sup>59</sup>

(58) K. L. Brown, L. Damm, J. D. Dunitz, A. Eschenmoser, R. Hobi, and C. Kratky, *Helv. Chim. Acta*, **61**, 3108 (1978).

(59) H. B. Bürgi and E. Shefter, *Tetrahedron*, **31**, 2976 (1975).

(60) J. J. Delpuech, G. Serratrice, A. Strich, A. Veillard, *Mol. Phys.*, **29**, 849 (1975).



common pattern, however (Figure 4). For comparison, ab initio calculations have been made for a simple model system, the  $\text{BH}_4^-$  anion with and without the electrostatic perturbation of a  $\text{Li}^+$  cation.<sup>61</sup> The calculations were limited to nuclear configurations with  $C_{3v}$  symmetry (15, 16). The deviations from  $T_d$  symmetry are then conveniently described<sup>62</sup> in terms of symmetry-adapted linear combinations of B-H bond lengths ( $r_i$ ) and HBH bond angles ( $\theta_{ij}$ ):

$$\begin{aligned} S_1(A_1) &= (r_1 + 3r_2 - 4r_0)/2 = t \\ S_{3a}(T_2) &= \sqrt{3}(r_1 - r_2)/\sqrt{2} = u \\ S_{4a}(T_2) &= \sqrt{3}(\theta_{12} - \theta_{23})/\sqrt{2} = v \end{aligned} \quad (3)$$

The deformation energy of the isolated  $\text{BH}_4^-$  anion was calculated up to cubic terms as a function of the symmetry coordinates  $t$ ,  $u$ , and  $v$ , which permits various constraint paths to be constructed (Figure 9). The effect of the electrostatic perturbation was calculated by minimizing the energy with respect to  $r_1$ ,  $r_2$ , and  $\theta_{12}$ , with the  $\text{Li}^+$  cation at fixed distances on either side of the anion; this gives the response path II, which lies between two constraint paths, III (obtained by constraining the  $u$  coordinate), and IV (by constraining the  $v$  coordinate). Of these three paths, the response path II is much the most similar to the experimental distribution of sample points for tetrahedral anions in different crystalline environments (Figure 4).

In summary, scattergrams of experimental structural data (Figures 1, 3, 4, and 5) may be interpreted as minimum-energy paths or as response paths. In the first interpretation, the correlations express a property characteristic solely of the structural fragment being investigated; in the second they express also effects of the environments that are imposed on the structural

(61) O. Eisenstein and J. D. Dunitz, *Isr. J. Chem.*, **19**, 292 (1980).

(62) P. Murray-Rust, H. B. Bürgi, and J. D. Dunitz, *Acta Crystallogr., Sect. B*, **B34**, 1787 (1978).

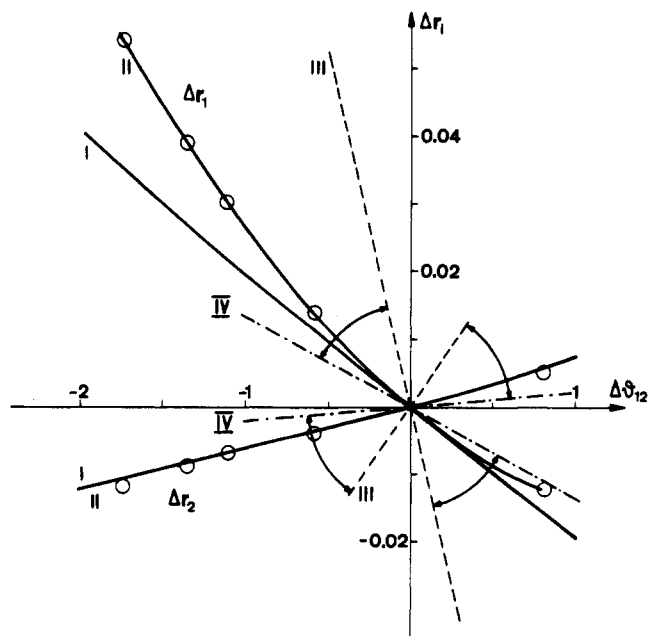


**Figure 9.** Dependence of  $\Delta r_1$ ,  $\Delta r_2$  (Å), and  $\Delta\theta_{12}$  (deg) for  $\text{BH}_4^-$  anion as expressed by various paths: I, regression curve from Figure 4;<sup>28</sup> II, calculated response path for electrostatic perturbation by  $\text{Li}^+$  cation (15, 16); III, IV calculated constraint paths with  $u$  and  $v$  (eq 3), respectively, as constraint coordinates.

fragment. The first interpretation will be more correct for narrow, steep-sided energy valleys, the second for wide, shallow valleys and relatively strong perturbations due to the environments. Any decision between these alternative interpretations cannot be made from crystallographic data alone, but will have to rely on additional information from a variety of possible sources: ab initio or molecular mechanics calculations, force constants from vibrational analysis, rotation barriers from temperature-dependent NMR studies, etc.

*It is a pleasure for both of us to thank the Swiss National Science Foundation for generous financial support over the years.*

## Calixarenes

C. DAVID GUTSCHE

Department of Chemistry, Washington University, St. Louis, Missouri 63130

Received August 12, 1982 (Revised Manuscript Received December 15, 1982)

The study of enzymes has occupied a central place in the physical and biological sciences for many years,

C. David Gutsche was born in La Grange, IL, in 1921. He received the B.A. from Oberlin College and the Ph.D. from the University of Wisconsin, working under the direction of W. S. Johnson. Since 1947 he has been a member of the faculty of Washington University, St. Louis, where he holds the rank of Professor. From 1970 to 1976 he served as chairman of the Department of Chemistry. His long-term research interests in diazoalkane-carbonyl reactions, ring-enlargement processes, and carbene chemistry changed in the 1970s to the areas of polyfunctional catalysts and enzyme mimics, one facet of which is portrayed in this Account.

and the catalytic prowess of these naturally occurring substances has long fascinated chemists. Only within the last two decades, however, have serious attempts been made to mimic the in vivo action of enzymes by means of simple in vitro chemical systems. Foremost among the compounds investigated for this purpose are the cyclodextrins, whose torus shape endows them with the ability to form host-guest complexes and, in certain cases, to act as powerful catalysts.<sup>1</sup> These compounds